

## Concentration-dependent Size Control of Germanium Nanocrystals

Louisa J. Hope-Weeks

Department of Chemistry and Biochemistry, Texas Tech University, Box 41061, Lubbock, Texas, 79409, U. S. A.

(Received July 26, 2005; CL-050966)

A room temperature solution phase preparation of germanium nanocrystals has been examined by means of varying the germanium precursor concentration. By varying the germanium tetrachloride concentration, it is possible to control the size distribution of nanocrystals formed.

Semiconductor nanocrystalline materials are a very active area of current research due to the dramatic change in properties of materials in the nanoscale compared to those observed in bulk materials.<sup>1,2</sup> Significant advances in the preparation and characterization of silicon nanocrystals,<sup>3–5</sup> porous silicon,<sup>6</sup> and II–VI semiconductors<sup>7</sup> and their novel size-dependent optical and electronic properties is widely documented.<sup>3,7–9</sup> However, there are substantially fewer reports on the preparation and characterization of porous germanium<sup>10</sup> and nanocrystalline germanium.<sup>11–16</sup> Physical procedures to produce germanium nanocrystals such as ion implantation,<sup>17</sup> gas evaporation,<sup>18</sup> chemical vapor deposition,<sup>19</sup> and laser annealing of amorphous material<sup>20</sup> are low yielding and the subsequent surface modifications are limited to that of either bare germanium, hydride, chloride, or oxide terminated surfaces.<sup>17–20</sup> Previously, documented solution phase preparation resulting in single nanometer sized germanium crystals often require extremely high pressures and high temperatures to induce crystallization.<sup>14,15,21</sup> Metathesis reactions using Zintl salt (KGe) precursors result in large size distributions (1–10 nm) and low yields, most likely due to the poor solubility of the precursor.<sup>11,12</sup> The use of inverse micelles to control crystal size is limited. Nucleation is not restricted to the hydrophilic interior of the micelle because of the solubility of GeCl<sub>4</sub> in hydrophobic region.<sup>16</sup> Recently, we reported a high yielding preparation of *n*-butyl capped germanium nanocrystals using an ambient temperature reduction of GeCl<sub>4</sub> with sodium naphthalide.<sup>22</sup> The size and shape of the nanocrystals were controlled by optimizing the growth period of the nanocrystals, with a longer growth time resulting in larger nanocrystals of 30–49 nm. The potential applications of semiconductor nanocrystals, such as biological sensing and tagging, requires tuning the optical or electronic properties therefore it is essential to produce nanocrystals with narrow size distributions in the 1–10 nm size region.

Here, a modified solution phase, low temperature preparation procedure resulting in germanium nanocrystals with discrete narrow size-distributions, is reported. The initial concentration of germanium is used to control sizes of nanocrystals formed in the reaction. Germanium nanocrystals with a discrete size distribution of 2–4 nm were produced by a sodium naphthalide reduction of germanium tetrachloride followed by surface modification with an excess of *n*-butyl lithium. A two fold increase in initial concentration of germanium tetrachloride produced germanium nanocrystals with a size distribution of 5–9 nm. In each case the nanocrystals formed as an orange, slightly oily solid which were soluble in dichloromethane (see Support-

ing Information).

The aliphatic regions of <sup>1</sup>H NMR spectra of both the 2–4 and 5–9 nm germanium nanocrystals in CDCl<sub>3</sub> were consistent with the presence of *n*-butyl groups on the surface of the nanocrystals. This is supported by the IR spectra, in which bands corresponding to C–H stretching of the alkyl groups were observed at ca. 3000 cm<sup>-1</sup>. A band corresponding to the Ge–O stretch at ca. 890 cm<sup>-1</sup>, was not present in the IR spectra, indicating that the surface was fully passivated.

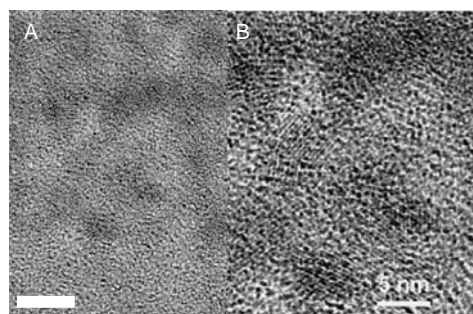


**Figure 1.** a) HR-TEM of 2–4 nm b) 6 nm *n*-butyl capped germanium nanocrystals on an ultra thin film carbon grid. Darker regions are germanium nanocrystals.

High-resolution transmission electron microscopy (HR-TEM) analysis of the 2–4 nm germanium nanocrystals on an ultra thin carbon grid is shown in Figure 1. To prepare the HR-TEM grids, a sample was suspended in dichloromethane and sonicated to solubilize the nanocrystals. The 2 nm ultra thin carbon grid was dipped into the solution and dried in an oven at 100 °C for 1.5 h. The size distribution was determined by measuring 450 nanocrystals from different areas on the grid. A histogram of the nanocrystal sizes is given in Figure 2a. A size distribution of 2–4 nm with 61% of the nanocrystals having a diameter of 3 nm was determined from this analysis. This narrow size distribution is a considerable improvement on those ob-

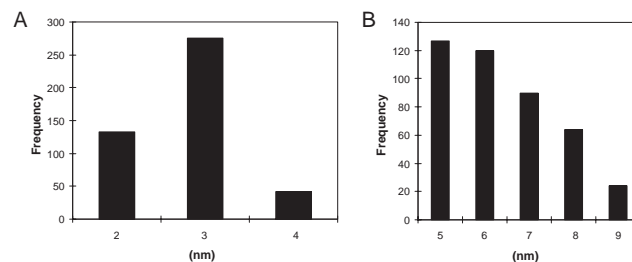


**Figure 2.** a) Histogram of 2–4 nm particle sizes from a survey of 450 nanocrystals from different regions of the grid. b) Histogram of 5–9 nm particle sizes from a survey of 425 nanocrystals from different regions of the grid.

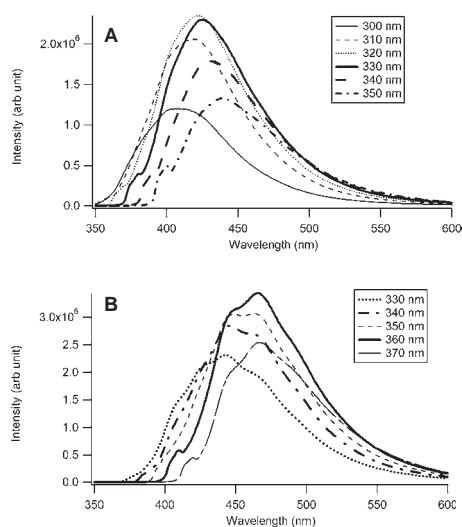


**Figure 3.** a) Size selective photoluminescence spectra 2–4 nm germanium nanocrystals. A smooth shift of emission wavelength with excitation wavelength is indicative of quantum confinement. b) Size selective photoluminescence spectra 5–9 nm germanium nanocrystals.

tained using previously reported solution preparation.<sup>11,12,16</sup> The HR-TEM image shows distinct lattice fringes of the nanocrystals, confirming their crystallinity.

The size distribution for the nanocrystals produced at higher initial germanium concentration was determined by measuring 425 nanocrystals from different areas on the grid. This analysis showed a size distribution of 5–9 nm with 58% of the nanocrystals falling in 5–6 nm range (Figure 2b). Figure 2b shows the HR-TEM image of a single nanocrystal of 6 nm where the lattice fringe spacing of 3.27 Å is consistent with (111) plane of germanium. This distribution is much narrower than those previously achieved using inverse micelle (1–10 nm) or metathesis reactions (1–10 nm).<sup>11,12,16</sup>

Figure 3a, shows the photoluminescence (PL) spectra for the 2–4 nm germanium nanocrystals which exhibit photoluminescence in a relatively narrow region of 420–430 nm with an excitation from 310–340 nm. A less intense region is resolved to 480 nm with excitation wavelengths of 350–380 nm. Figure 3b, shows the PL spectra for the 5–9 nm germanium nanocrystals which exhibit photoluminescence in a relatively narrow region of 450–470 nm with an excitation of 330–360 nm. A less intense region is resolved to 500 nm with excitation wavelengths from 370–410 nm, which is consistent with previously reported studies and with the quantum confinement model.<sup>11,12,16</sup>

In conclusion, the initial concentration of germanium can be

used to control the size of nanocrystals formed in the solution phase, resulting in two discrete narrower size distributions than previously published procedures.<sup>11,12,16</sup> Future work will optimize these conditions, to further control the size distribution of germanium nanocrystals.

We thank the imaging center assistance with the TEM.

## References

- 1 M. A. El-Sayed, *Acc. Chem. Res.*, **37**, 326 (2004).
- 2 T. J. Bukowski and J. H. Simmons, *Crit. Rev. Solid State*, **27**, 119 (2002).
- 3 J. P. Wilcoxon, R. L. Williamson, and R. J. Baughman, *Chem. Phys.*, **98**, 9933 (1993).
- 4 R. K. Baldwin, K. A. Pettigrew, E. Ratai, M. P. Augustine, and S. M. Kauzlarich, *Chem. Commun.*, **2002**, 1822.
- 5 R. K. Baldwin, K. A. Pettigrew, J. C. Garno, P. P. Power, G. Liu, and S. M. Kauzlarich, *J. Am. Chem. Soc.*, **124**, 1150 (2002).
- 6 M. J. Sailor and K. L. Kavanagh, *Adv. Mater.*, **4**, 432 (1992).
- 7 J. R. Heath and J. Shiang, *J. Chem. Soc. Rev.*, **27**, 65 (1998).
- 8 Y. Wang and N. Herron, *J. Phys. Chem.*, **95**, 525 (1991).
- 9 C. J. Murphy and J. L. Coffey, *Appl. Spectrosc.*, **56**, 16A (2002).
- 10 S. Miyazaki, K. Sakamoto, K. Sheba, and M. Hirose, *Thin Solid Films*, **255**, 99 (1995).
- 11 B. R. Taylor, S. M. Kauzlarich, G. R. Delgado, and H. W. H. Lee, *Chem. Mater.*, **11**, 2493 (1999).
- 12 B. R. Taylor, S. M. Kauzlarich, G. R. Delgado, and H. W. H. Lee, *Chem. Mater.*, **10**, 22 (1998).
- 13 S.-T. Ngiam, K. F. Jensen, and K. D. Kolenbrander, *J. Appl. Phys.*, **76**, 8201 (1994).
- 14 J. R. Heath and F. K. LeGoues, *Chem. Phys. Lett.*, **208**, 263 (1993).
- 15 J. R. Heath, J. J. Shiang, and A. P. Alivisatos, *J. Chem. Phys.*, **101**, 1670 (1994).
- 16 J. P. Wilcoxon, P. P. Provencio, and G. A. Samara, *Phys. Rev. B*, **64**, 035417 (2001).
- 17 K. S. Min, K. V. Shcheglov, C. M. Yang, H. A. Atwater, M. L. Brongersma, and A. Polman, *Appl. Phys. Lett.*, **68**, 2511 (1996).
- 18 C. Bostedt, T. Van Buuren, J. M. Plitzko, T. Moller, and L. J. Terminello, *J. Phys.: Condens. Matter*, **15**, 1017 (2003).
- 19 A. K. Dutta, *Appl. Phys. Lett.*, **68**, 1189 (1996).
- 20 A. Kornowski, M. Giersig, R. Vogel, A. Chemseddine, and H. Weller, *Adv. Mater.*, **5**, 634 (1993).
- 21 D. Gerion, N. Zaitseva, C. Saw, M. F. Casula, S. Fakra, T. Van Buuren, and G. Galli, *Nano Lett.*, **4**, 597 (2004).
- 22 L. J. Hope-Weeks, *Chem. Commun.*, **2003**, 2980.